

Supporting information for:

Ni-Doped ZrO₂ nanoparticles decorated MW-CNTs
nanocomposite for highly sensitive electrochemical
detection of 5-amino salicylic acid

Nandini Nataraj,^a Siva Kumar Krishnan,^b Tse-Wei Chen,^{a,c,d} Shen-Ming Chen,^{*a}

Bih-Show Lou^{*e,f}

^aDepartment of Chemical Engineering and Biotechnology, National Taipei University of
Technology, No.1, Section 3, Chung-Hsiao East Road, Taipei 106, Taiwan.

^bCONACYT-Instituto de Física, Benemérita Universidad Autónoma de Puebla, Apdo.
Postal J-48, Puebla 72570, Mexico.

^cResearch and Development Center for Smart Textile Technology, National Taipei
University of Technology, Taipei 106, Taiwan, ROC.

^dDepartment of Materials, Imperial College London, London, SW7 2AZ, United
Kingdom.

^eChemistry Division, Center for General Education, Chang Gung University, Taoyuan
333, Taiwan.

^fDepartment of Nuclear Medicine and Molecular Imaging Center, Chang Gung Memorial
Hospital, Taoyuan 333, Taiwan

Corresponding author:

S.-M. Chen, Email: smchen78@ms15.hinet.net Tel: +886 2270 17147, Fax: +886
2270 2523;

B.-S. Lou, Email: blou@mail.cgu.edu.tw Tel: +886 3211 8800, Fax: +886 3211 8700

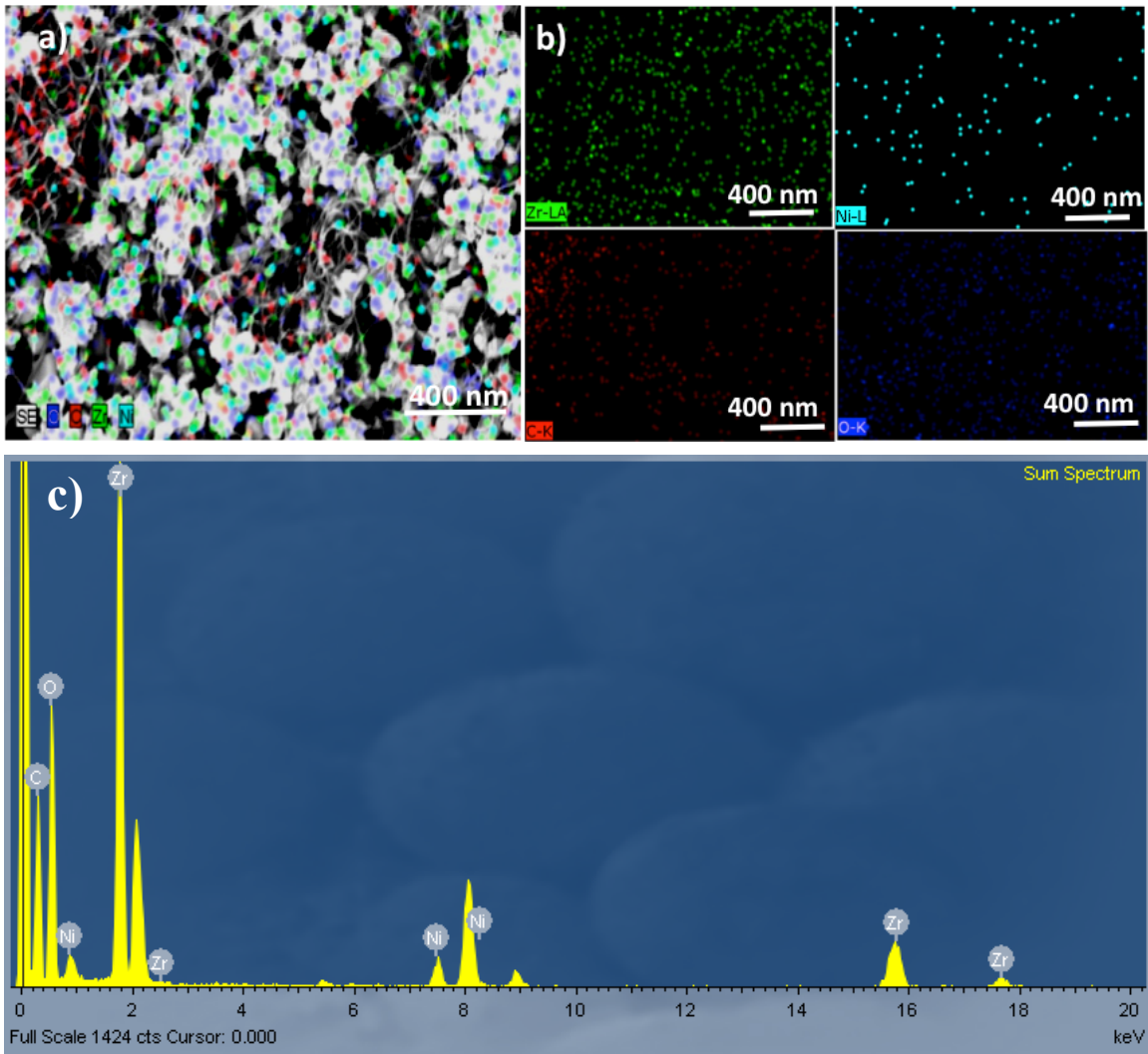


Fig S1. (a, b) EDX-elemental mapping analysis of Ni-ZrO₂/MWCNT nanocomposite, (c) EDX-elemental spectrum analysis of Ni-ZrO₂/MWCNT nanocomposite.

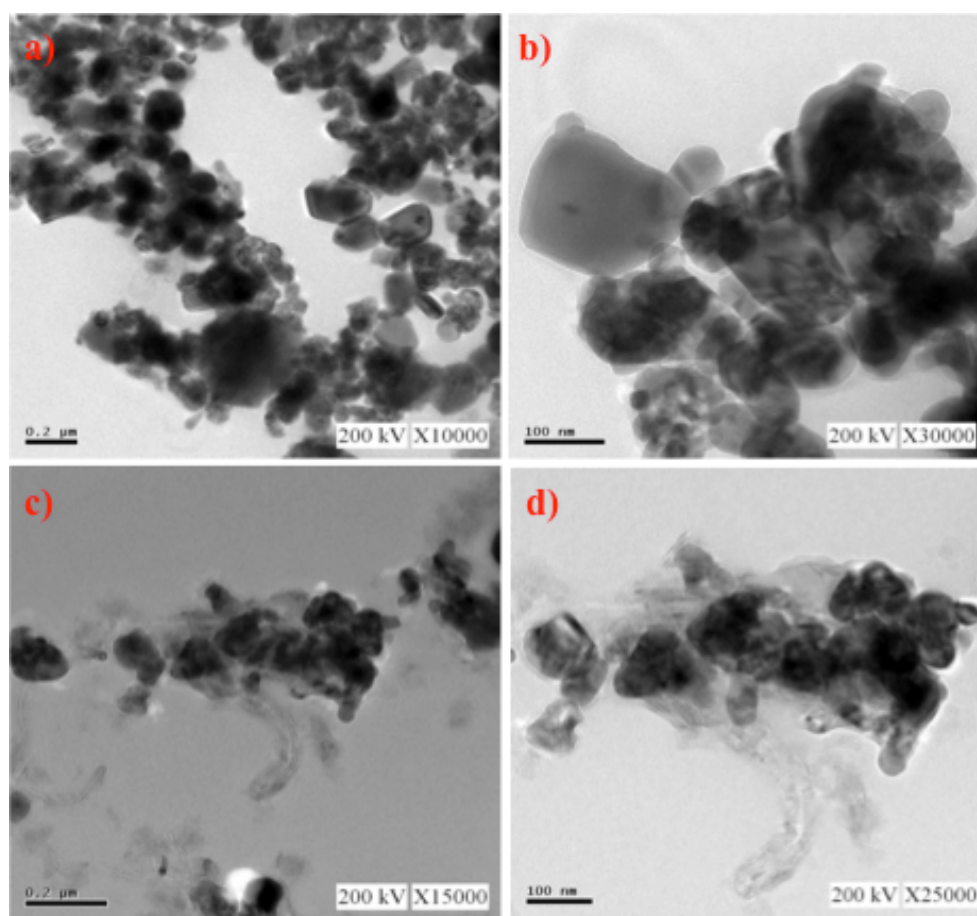


Fig S2. TEM images of a, b) Ni-ZrO₂ NPs, c, d) Ni-ZrO₂/MWCNT nanocomposite.

Estimation of Electrochemically active surface area (EASA) behavior of various electrodes

The EASA values were determined using the Randles–Sevcik equation is shown in equ (1):

$$I_{pa} = (2.69 \times 10^5) n^{3/2} A C D^{1/2} v^{1/2} \dots\dots\dots (1)$$

Where I_p is the peak current, D is the diffusion coefficient of the ferricyanide solution, A is the active surface area of the electrode, n is the number of electrons involved in the reaction, C is the concentration of the ferricyanide solution, v is the scan rate (Vs^{-1}). The calculated EASA for the bare GCE, Ni-ZrO₂-GCE, MWCNT/GCE, and Ni-ZrO₂/MWCNT/GCE was about 0.080, 0.278, 0.182, and 0.313 cm², respectively.

In addition, the redox properties of the modified electrodes were studied in 0.1 M Ru(NH₃)₆]^{3+/2+} containing 0.5 M KCl at a scan rate of 50 mV s⁻¹. As can be seen in the **Fig S3a**, all the electrodes exhibit the apparent redox peaks in the measured potential range due to the transfer of [Ru (NH₃)₆]²⁺ to [Ru (NH₃)₆]³⁺. The bare GCE shows the low redox peak current along with broad peak-to peak potential separation (ΔE_p). After GCE is modified with bare Ni-ZO₂, MWCNTs, and Ni-ZrO₂/MWCNT, the peak current increased and the ΔE_p ratio is gradually decreased, which is due to the increased diffusion pathways, improved electrical conductivity, and rapid electron transfer in the electrode surface. The Ni-ZrO₂/MWCNT/GCE exhibits lower ΔE_p separation of 143 mV with higher current response than the other modified and bare electrodes; suggest that the modified electrodes are highly reversible reaction process. In addition, **Fig. S3b** displays the CV curves of Ni-ZrO₂/MWCNT/GCE obtained by varying the scan rate from 20 to 200 mV s⁻¹ in 0.1 M Ru(NH₃)₆]^{3+/2+} containing 0.5 M of KCl solution. As can be seen in **Fig S3b**, the redox peak current response increased with increasing the scan rate from 20

to 200 mVs^{-1} . A linear plot was obtained between the redox currents and square root of scan rate as shown in **Fig S3c**. These results further suggest that the excellent electrochemical redox activity of Ni-ZrO₂/WCNT/GCE, which is consistent with the results obtained in $[\text{Fe}(\text{CN})_6]^{3-/4-}/\text{KCl}$ (**Fig 3b-d**).

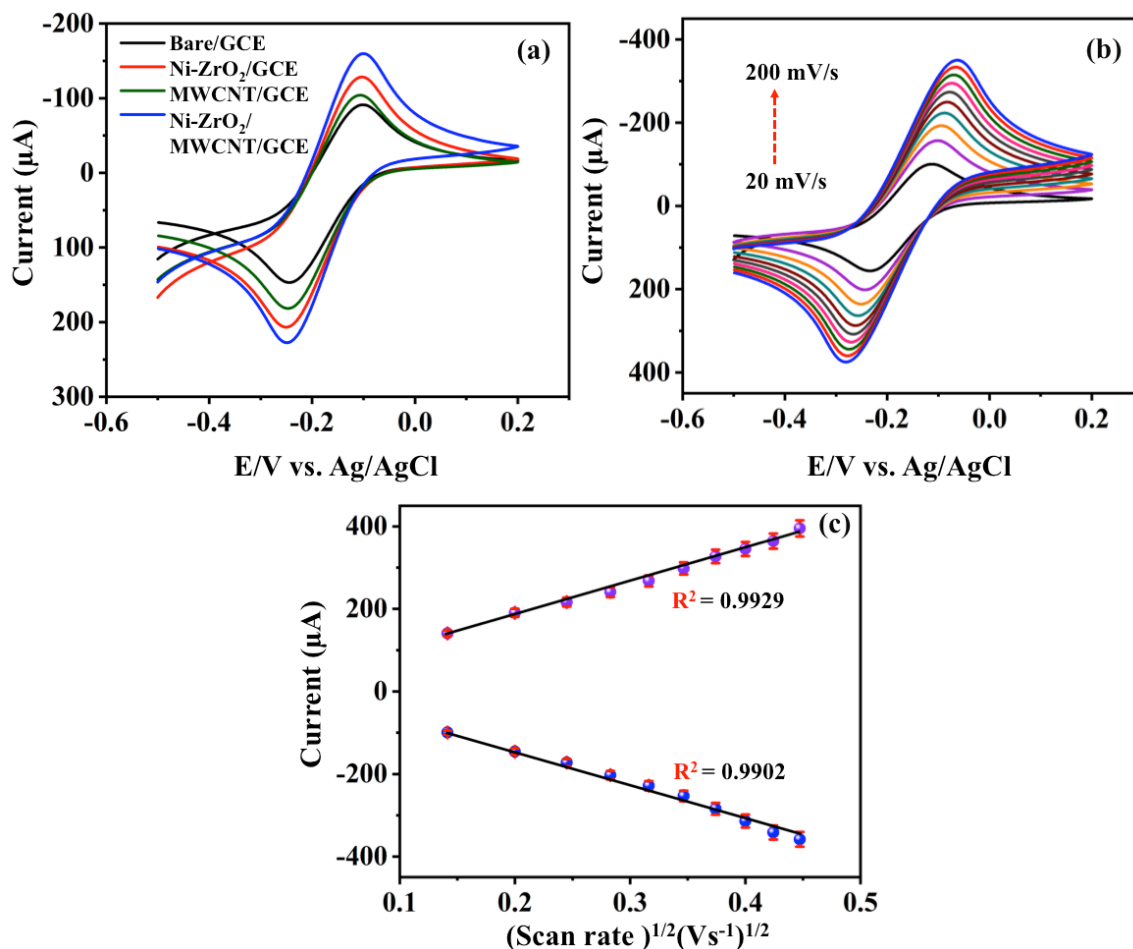


Fig S3. a) CV curves of the modified electrodes in 0.1 M of $[\text{Ru}(\text{NH}_3)_6]^{3+/2+}$ mixed 0.5 M of KCl solution at a sweep rate of 50 mV s^{-1} . b) CV curves at different scan rates of the Ni-ZrO₂/MWCNT/GCE in 0.1 M $[\text{Ru}(\text{NH}_3)_6]^{3+/2+}$ mixed 0.5 M of KCl. c) linear calibration for a redox peak current response vs square root of scan rate.

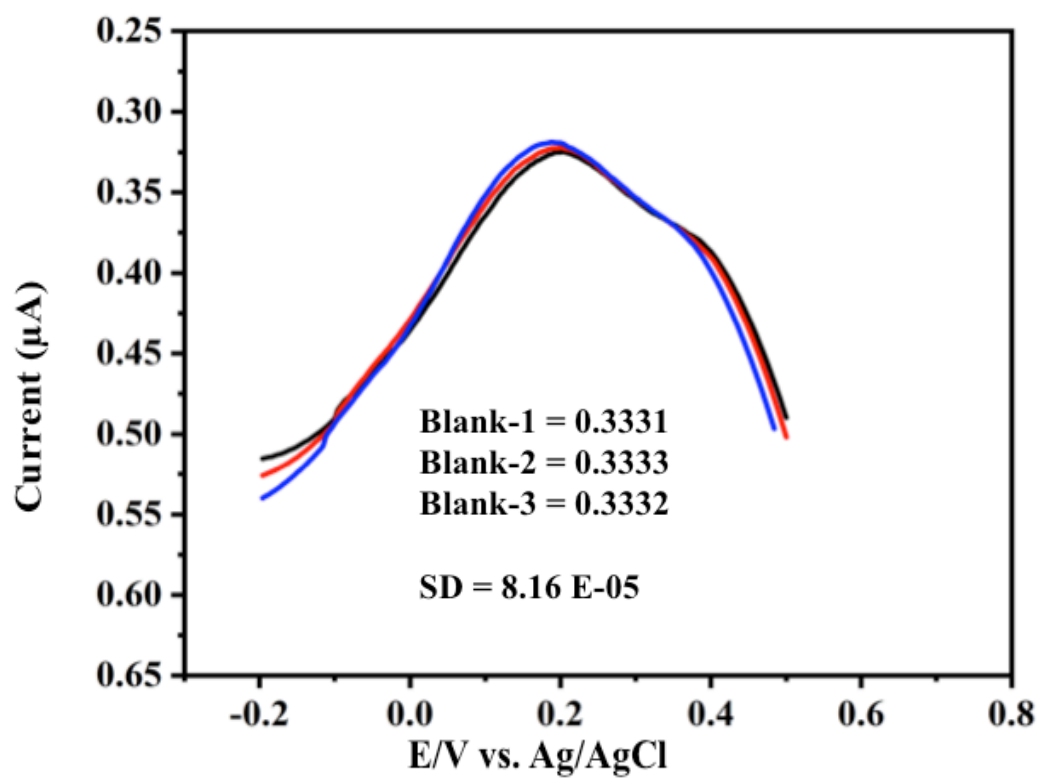


Fig S4. Electrochemical response of three blank samples

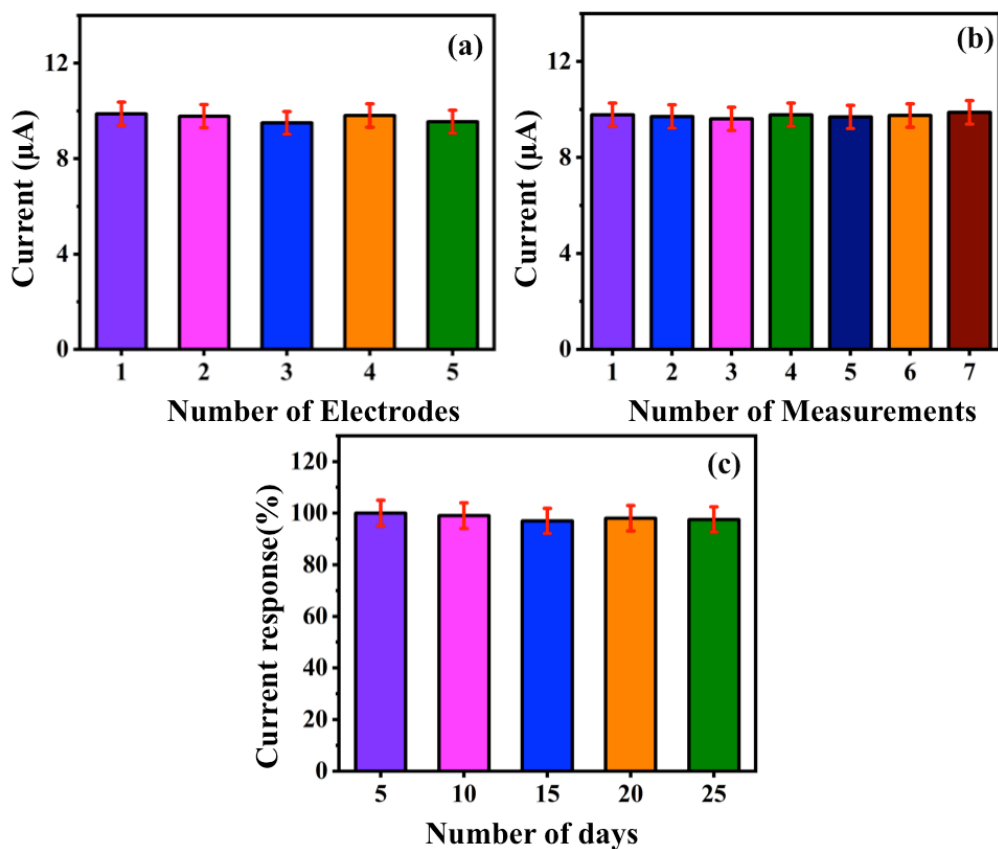


Fig S5. (a) Reproducibility, (b) Repeatability, and (c) Stability analysis of Ni-ZrO₂/MWCNT-modified GC electrode.

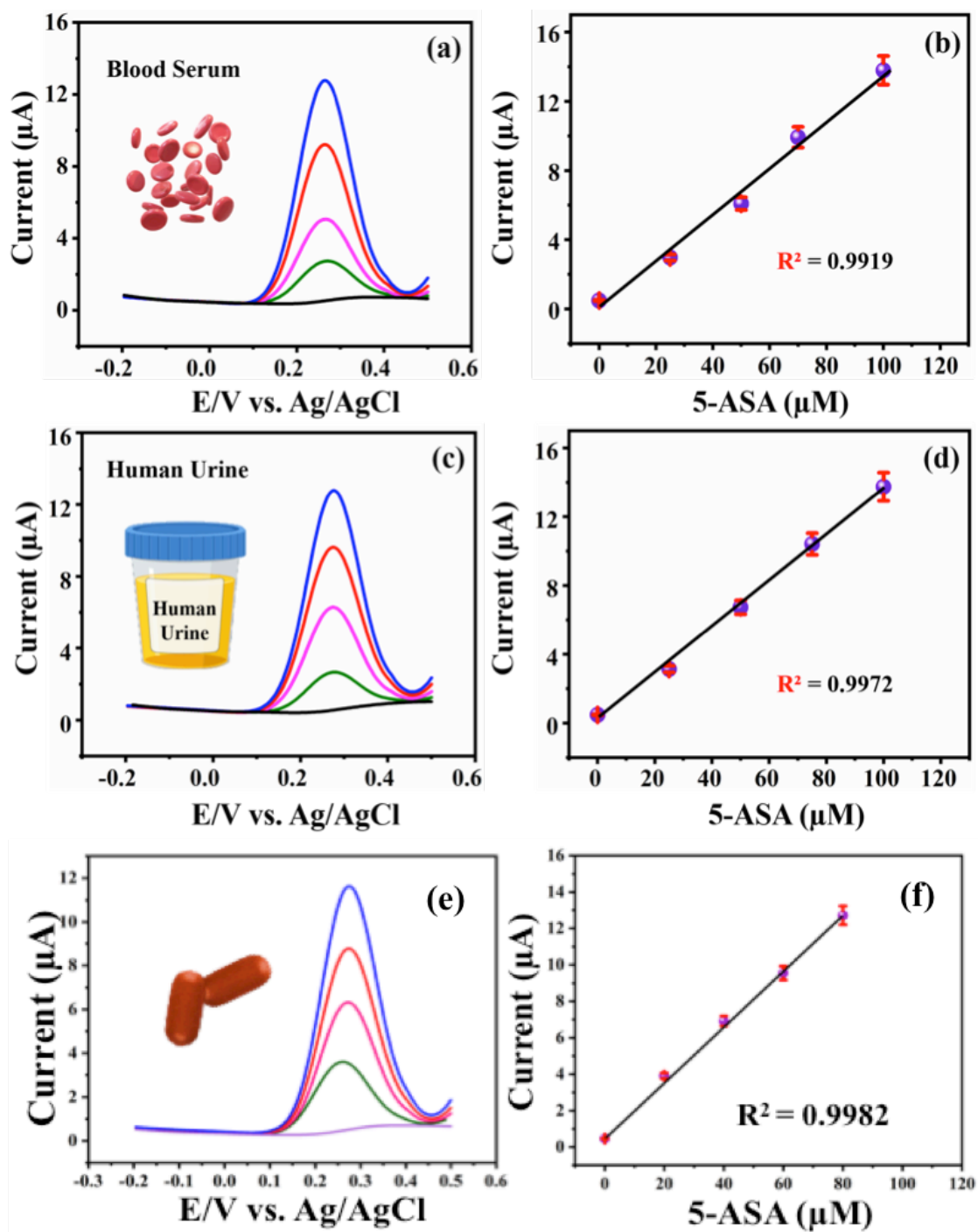


Fig S6. (a) The DPV responses for real-time detection of 5-ASA in blood serum (a), human urine (c), and 5-ASA tablets (e) at Ni-ZrO₂/MWCNT/GCE with PBS (0.1 M, pH=7.0), (b, d, f) Corresponding calibration plot of I_{pa} vs 5-ASA concentration.